

THz absorption spectra of akaganeite (β -FeOOH), lepidrocite (γ -FeOOH) and bernalite ($\text{Fe}(\text{OH})_3$)

Ryo Hasegawa^{1*}, Takashi Kimura¹, Tadao Tanabe¹, Katsuhiko Nishihara², Akira Taniyama² and Yutaka Oyama¹

¹Department of Materials Science and Engineering, Tohoku University, Aramaki Aza Aoba 6-6-11-1020, Sendai 980-8579, Japan

²Nippon Steel and Sumitomo Metal Co., Ltd. 1-8 Fuso-Cho, Amagasaki, Hyogo, 660-0891 Japan

*Corresponding author: Ryo Hasegawa, Department of Materials Science, Graduate School of Engineering, Tohoku University, Aramaki-Aza Aoba 6-6-11-1021, Sendai 980-8579, Japan, Tel: +81-22-795-7330; Fax: +81-22-795-7329; E-mail: ryo.hasegawa.p8@tohoku.ac.jp

Received date: July 31, 2018; Accepted date: August 30, 2018; Published date: September 9, 2018

Copyright: © 2018 Hasegawa R, et al. This is an open-access article distributed under the terms of the Creative Commons Attribution License, which permits unrestricted use, distribution, and reproduction in any medium, provided the original author and source are credited.

Abstract

Nonpolar substances have high transparency for both THz and radio waves, and THz waves are reflected from metal surfaces as efficiently as light waves. These characteristics are advantageous in applying THz waves in various fields, including non-destructive, non-contact inspection. Our research is aimed at non-destructive, non-contact inspection of hot-dip galvanized steel sheet using THz imaging. We have conducted terahertz spectroscopic analysis of goethite (α -FeOOH), which can be present on hot-dip galvanized steel sheet. In this paper, with the intention of developing further practical applications, we investigated the THz spectra of akaganeite (β -FeOOH), lepidrocite (γ -FeOOH) and bernalite ($\text{Fe}(\text{OH})_3$) in the expanded frequency range from 1.0 to 6.0 THz generated by a GaP crystal, and from 8.4 to 11.0 THz with the addition of a newly fabricated GaSe crystal. In addition, Attenuated Total Reflectance (ATR) FTIR spectral measurements were conducted and the results were compared with the results from the monochromatic terahertz spectroscopic analyses.

Keywords Terahertz; Metal corrosion; NDT; Infrared active; Non-destructive imaging

Introduction

Terahertz waves are in the frequency range from about 0.1 to 10 THz (1THz=10¹²Hz), with corresponding wavelengths of 30 to 3000 μm . This was an undeveloped frequency region because it was very difficult to generate and detect electromagnetic radiation at these frequencies. However, in recent years, it has become possible to do this and it is expected that terahertz waves will be applied in wireless communications, non-destructive imaging (NDT), and identification of materials by fingerprint vibration spectra. One of the characteristics of terahertz waves is that the wavelength is longer than that of visible and/or infrared light, and the quantum photon energy is very small, and thus is safe for human tissue. This energy of terahertz waves corresponds to that of the intramolecular vibrations of several substances. Therefore, when we can find absorption peaks, we can use terahertz waves as an identification tool using intermolecular vibration analysis. Our group has created a database of THz permeability characteristics for industrial materials, and successfully constructed non-destructive THz diagnosis of building blocks [1-2], insulated copper cable [3], hot-dip galvanized steel sheet [4] and aqueous solution of glucose and chocolate [5,6]. Furthermore, the energy of a THz wave corresponds to molecular interactions such as hydrogen bonding, van der Waals interactions and lattice interactions. The lattice interaction is affected by a mechanical deformation of polymer. THz spectroscopy can be used for non-destructive diagnosis of mechanical deformation in polymers [7]. In addition, terahertz waves are located between radio waves and light waves, so they have the transmission characteristics of radio waves in nonpolar substances and the reflection characteristics of light waves at metal surfaces. Thus, if we have a metal coated with an opaque film, THz waves can pass through the film and

be reflected at the metal surface allowing us to determine the state of the metal under the coating without the need to peel the coating [8]. So non-destructive, non-contact inspection can really be performed using THz waves. Especially, in this paper, we are aiming for the nondestructive inspection of hot-dip galvanized steel sheet. Hot-dip galvanized steel sheet is a plated steel sheet that has both light weight and high strength, and is widely used for car bodies and as a building material. Normally, the iron surface is protected by a plating layer, but when the plating layer is damaged, iron-based corrosion products can be generated. The iron-based corrosion products begin with the formation of bernalite ($\text{Fe}(\text{OH})_3$), then branches to goethite (α -FeOOH) or akaganeite (β -FeOOH) or γ -FeOOH depending on the environment and finally becomes hematite (α -Fe₂O₃). Therefore, if each iron hydroxide corrosion product on the plated steel sheet can be quantitatively and qualitatively inspected in real time, it is possible to determine the corrosion process of the plated steel sheet and track the corrosion step. In our previous studies, we conducted terahertz spectroscopic analysis of goethite (α -FeOOH), which may be present on hot-dip galvanized steel sheet, and the existence of an absorption peak due to infrared activity was clarified [9]. From those results, the absorption peak at 10.25 THz was considered to be due to intramolecular vibrations. Conversely, the remaining absorption peaks, at 9.85, 9.95 and 10.15 THz, were considered to be due to intermolecular vibrations. In this paper, with the aim of creating further practical applications, we investigated the THz spectra of akaganeite (β -FeOOH), lepidrocite (γ -FeOOH) and bernalite ($\text{Fe}(\text{OH})_3$) in the expanded frequency range from 1.0 to 6.0 THz, generated by a GaP crystal, and from 8.4 to 11.0 THz, generated by a GaSe crystal. In addition to the THz spectroscopic analysis, Attenuated Total Reflectance (ATR) FTIR spectral measurements were conducted and each spectrum is compared and discussed.

Materials and Methods

Sample preparation

γ -FeOOH and $\text{Fe}(\text{OH})_3$ were purchased from Japan Pure Chemical Co., Ltd. β -FeOOH was obtained by adding sodium hydroxide dropwise to iron chloride. Each corrosion powder sample was diluted with polyethylene powder which has high permeability to terahertz waves. In order to obtain quantitative relationships for the absorption peaks, sample mixing ratios of 1.0, 3.0, 5.0 and 10.0 weight percent were used. The diameter and thickness of the pellets were 20 mm and less than 1mm, respectively. The pellets were compressed at a pressure of 1.0 ton/cm² for 1 min and tilted at 2° during the measurements to prevent interference. Details of the corrosion powder samples used in the pellets is shown in Table 1.

	Molecular Weight	Purity
β -FeOOH	88.85	Unmeasured
γ -FeOOH	88.85	>99%
$\text{Fe}(\text{OH})_3$	106.87	>99%

Table 1: Details of the corrosion powder samples

Optical system for the THz spectrometer

The detailed experimental set up for the THz spectrometer has been described in previous reports [10,11]. The optical system in the range from 1.0 to 6.0 THz is shown in Figure 1.

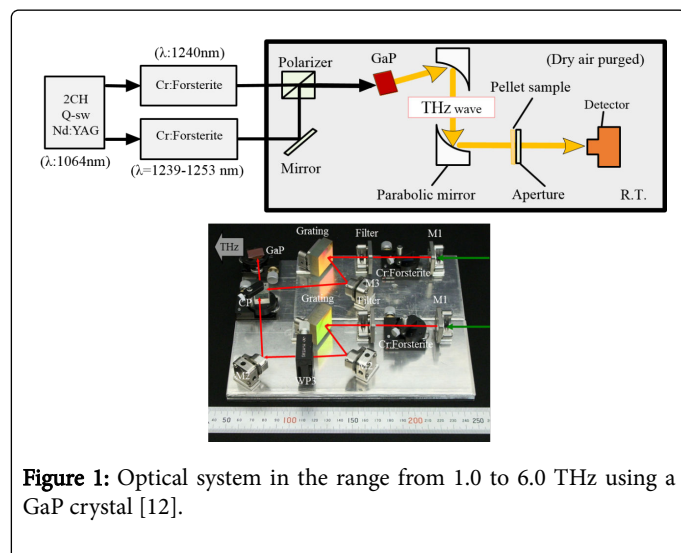


Figure 1: Optical system in the range from 1.0 to 6.0 THz using a GaP crystal [12].

The probe beam is produced by a frequency variable Cr:Forsterite laser excited by a Nd:YAG laser. Two different frequencies close to the infrared region are introduced into the GaP crystal. The THz waves generated are directed toward the sample pellet and detected by DTGS or a 4.2 K Si bolometer depending on the absorption efficiency of the material. The linewidth of the THz radiation is about 20 GHz. The optical system in the range from 8.4 to 11.0 THz has been described in a previous report [9].

ATR-FTIR Spectroscopy

The equipment used for ATR-FTIR spectroscopy was the same as the one previously used for α -FeOOH [9]. The measurements were carried out in the range of 100 cm⁻¹-4000 cm⁻¹ (3.0-12.0 THz) in the far-infrared region at room temperature. The absorption peaks obtained by ATR-FTIR are shown in Figure 2.

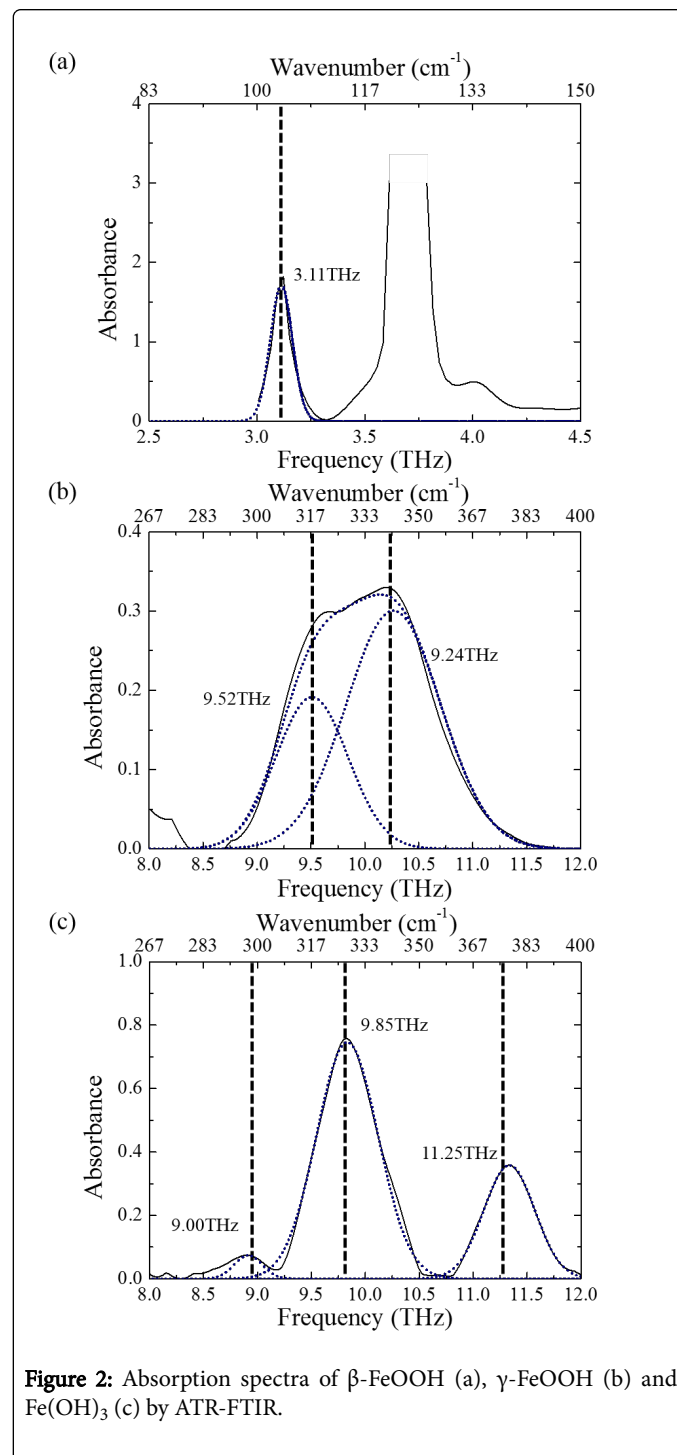


Figure 2: Absorption spectra of β -FeOOH (a), γ -FeOOH (b) and $\text{Fe}(\text{OH})_3$ (c) by ATR-FTIR.

In the measurements of β -FeOOH, one sharp absorption peak was clearly obtained in the low frequency region generated in the GaP crystal. In the measurement of γ -FeOOH, two absorption peaks with

broad full widths at half maximum (FWHM) were obtained. In $\text{Fe}(\text{OH})_3$, one weak absorption peak and two strong absorption peaks were observed. Because higher resolution can be expected with terahertz spectroscopy, this can help us clarify the absorption peaks and assign them in this case. In terahertz wave spectroscopy, measurement with higher resolution is possible. The frequency resolution of the GaP crystal is 20GHz and that of the GaSe crystal is 500MHz, so these results can assist the results obtained with terahertz wave spectroscopy.

Results and Discussion

The absorption peaks obtained with THz spectroscopy are shown in Figure 3.

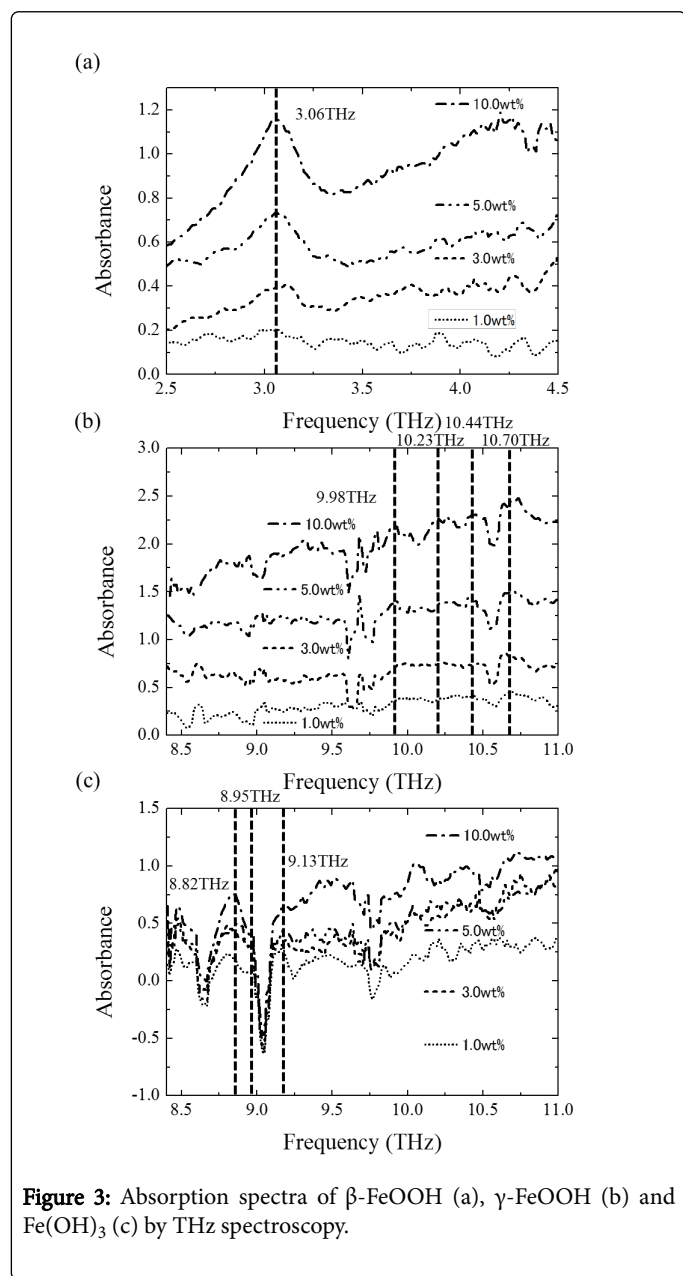


Figure 3: Absorption spectra of β -FeOOH (a), γ -FeOOH (b) and $\text{Fe}(\text{OH})_3$ (c) by THz spectroscopy.

In the measurement of β -FeOOH, a clear absorption peak was obtained at 3.06 THz. This peak can be considered to be assigned to

the peak at 3.11 THz obtained by ATR-FTIR. In the measurement of γ -FeOOH, weak absorptions were obtained at 9.98 THz, 10.23 THz, 10.44 THz and 10.70 THz. On the other hand, absorption peaks were obtained at 9.52 THz and 9.24 THz in the ATR-FTIR measurement. Although the number of absorption peaks obtained is different, it is considered that all the absorption peaks obtained by terahertz spectroscopy can be assigned to the peaks obtained by ATR-FTIR. The frequency resolution obtained by THz spectroscopy in our research group is higher than the frequency resolution obtained by ATR-FTIR. Therefore, in the results, there is a possibility that small peaks with small FWHMs not detected by ATR-FTIR are visible. In the same way, in the measurement of $\text{Fe}(\text{OH})_3$, absorption peaks at 8.82 THz, 8.98 THz and 9.13 THz were obtained, and these peaks are considered to be attributed to the 9.00 THz or 9.85 THz peaks in the ATR-FTIR measurements. Also, in the ATR-FTIR results for $\text{Fe}(\text{OH})_3$, the absorption peaks obtained at 9.85 THz and 11.25 THz were not obtained by terahertz spectroscopy. We think that the terahertz waves generated in the GaSe crystal at this frequency are weak, so the peaks are buried in the noise. The obtained absorption peaks, including the absorption peak in α -FeOOH measured previously, are summarized in Table 2.

Powder samples	THz spectroscopy(THz)	ATR-FTIR (THz)
α -FeOOH	9.85	9.95
	9.95	
	10.15	
	10.25	10.54
β -FeOOH	3.06	3.11
		11.38
γ -FeOOH	9.98	9.52
	10.23	9.24
	10.44	
	10.7	
$\text{Fe}(\text{OH})_3$	8.82	9.00
	8.95	
	9.13	
		9.85
		11.25

Table 2. Absorption peaks due to the infrared activity of iron hydroxide corrosion products.

In terahertz spectroscopy, it is possible to see peaks which have small FWHM that cannot be seen by ATR-FTIR.

Conclusion

In this study, the absorption peaks due to the infrared activity of akaganeite (β -FeOOH), lepidrocite (γ -FeOOH) and bernalite ($\text{Fe}(\text{OH})_3$) were obtained by THz spectroscopy and ATR-FTIR. The absorption peaks obtained in mutual spectra are in agreement, and it demonstrates that higher resolution spectrum can be obtained using

THz waves generated by the difference frequency generation (DFG) method. Also, since THz imaging uses a fixed frequency wave, the absorption peak in THz spectroscopy is considered to be superior to that of ATR-FTIR. As the terahertz wave database for iron based corrosion products becomes established in the higher THz frequency region, THz spectroscopic imaging of invisible corrosion products can be expected even for steel plate under an opaque coating.

Acknowledgment

This study is partially supported by “Fundamental Research and Human Resources Development Program for Nuclear Decommissioning related to Integrity Management of Critical Structures including Primary Containment Vessel and Reactor Building, and Fuel Debris Processing and Radioactive Waste Disposal” carried out under the Center of World Intelligence Project for Nuclear S&T and Human Resource Development by the Ministry of Education, Culture, Sports, Science and Technology of Japan.

References

1. Oyama Y, Zhen L, Tanabe T, Kagaya M (2009) Sub-terahertz imaging of defects in building blocks. *NDT E Int* 42: 28–33.
2. Tanabe T, Kanai T, Kuroo K, Nishiwaki T, Oyama Y (2018) Non-contact Terahertz Inspection of Water Content in Concrete of infrastructure buildings. *World J Eng Technol* 6: 268-274.
3. Takahashi S, Hamano T, Nakajima K, Tanabe T, Oyama Y (2014) Observation of damage in insulated copper cables by THz imaging. *NDT E Int* 61: 75–79.
4. Nakamura Y, Kariya H, Sato A, Tanabe T, Nishihara K, et al. (2014) Nondestructive corrosion diagnosis of painted hot-dip galvanizing steel sheets by using THz spectral imaging. *Corros Eng* 63: 411–416.
5. Torii T, Chiba H, Tanabe T, Oyama Y (2017) Measurements of glucose concentration in aqueous solutions using reflected THz radiation for applications to a novel sub-THz radiation non-invasive blood sugar measurement method. *Digit Health* 3: 1-5.
6. Weiller S, Tanabe T, Oyama Y (2018) Terahertz Non-contact Monitoring of Cocoa Butter in Chocolate. *World J Eng Technol* 6: 275-281.
7. Tanabe T, Watanabe K, Oyama Y, Seo K (2010) Polarization sensitive THz absorption spectroscopy for the evaluation of uniaxially deformed ultra-high molecular weight polyethylene. *NDT E Int* 43: 329–333.
8. Nakamura Y, Kariya H, Sato A, Tanabe T, Nishihara K, et al. (2014) Non-destructive Corrosion Diagnosis of Painted Hot-dip Galvanizing Steel Sheets by Using THz Spectral Imaging. *Corros Eng* 63: 504-509.
9. Hasegawa R, Kimura T, Tanabe T, Nishihara K, Taniyama A et al. (2018) Analysis of the specific vibration modes of goethite (α -FeOOH) by terahertz spectroscopy and calculations of the vibration frequencies of a single molecule using density functional theory. *J Biomed Graph Comput* 8: 29.
10. Suto K, Sasaki T, Tanabe T, Kimura T (2005) Gap THz wave generator and THz spectrometer using Cr:Forsterite lasers. *Rev Sci Instrum* 76: 123109.
11. Nishizawa J, Suto K, Sasaki T, Tanabe T, Kimura T (2003) Spectral measurement of terahertz vibrations of biomolecules using a GaP terahertz-wave generator with automatic scanning control. *J Phys D: Appl Phys* 36: 2958-2961.
12. Tanabe T, Oyama Y (2011) Frequency-Tunable Coherent THz-Wave Pulse Generation Using Two Cr:Forsterite Lasers with One Nd:YAG Laser Pumping and Applications for Non-Destructive THz Inspection. *Laser Syst Applications* 119-136.